Chemical Science

EDGE ARTICLE

View Article Online
View Journal | View Issue

Cite this: *Chem. Sci.*, 2018, **9**, 1481

Synthesis of stable polymetalated aromatic complexes through metal–macrocycle capsule-triggered cyclization†

Xin He,[a] Yang Xue,[a] Cui-Cui Li,[a] Yuechao Wang,[b] Hong Jiang[b] and Liang Zhao*[a]

Received 17th October 2017
Accepted 2nd December 2017

DOI: 10.1039/c7sc04503d

rsc.li/chemical-science

Polymetalated aromatic compounds are of great interest because of their intermediate roles in many organic transformations. However, they are elusive and synthetically challenging. In this study, a dynamic coordination capsule constructed by a flexible macrocycle and silver(I) ions is applied to trigger one-step or cascade cyclization reactions for various alkyne substrates, finally leading to five unprecedented polysilver heteroaromatic intermediates (including indole, quinoline, benzocarbazole and 2,2′-biindole). The acquired heteroaromatic species is doubly charged, particularly at vicinal positions, and each is surrounded by a tetrasilver aggregate. The metal–macrocycle capsule holds a great potential of flexibly adjusting its conformation to adapt different polysilver heteroaromatic species. DFT calculations further reveal that metal-perturbed aromaticity and multi-centered bonding both contribute to stabilization of the polysilver heteroaromatic complexes.

Introduction

Inspired by enzymes' remarkable ability to control and manipulate chemical reactions by means of steric confinement and precisely positioned functional groups, in the past decades chemists have made many attempts to mimic desirable properties of protein catalysts by constructing a confined environment *via* a molecular container.[1] Besides covalently linked cyclic or cage-like molecules,[2] recent preparation of molecular containers has evolved to more complex and elegant self-assembled architectures relying on the association of easily accessible modular components *via e.g.* metal–ligand coordination.[3] The container architectures can encage guest molecules within a confined space, dynamically harness multiple non-covalent interactions in a synergistic manner to stabilize highly reactive transition states of substrate molecules, and accelerate otherwise sluggish chemical reactions. A variety of reactions (*e.g.* Diels–Alder reaction,[4] electrocyclization,[5] photoaddition[6] and reductive elimination[7]) have been performed within metallacage hosts, yielding products with unusual selectivity and/or enhanced activity. However, yet to date there are few precedent examples of supramolecular coordination capsules that exhibit sufficient structural flexibility to adapt diverse substrates by adjusting cavity size.[8] In addition, structurally well-defined reaction intermediates in the cavity of supramolecular coordination capsules are rarely isolated.

On the other hand, polymetalated organometallic compounds are of great interest to synthetic chemists due to their promising potential for the synthesis of multi-substituted aromatic compounds,[9] and their special role in the comprehension of reaction mechanisms provides inspiration for developing new synthetic methodologies.[10] However, these kinds of compounds are challenging synthetic goals because of the difficulty of generating polyanionic species by direct electrophilic metalation or halogen–lithium–metal exchange reactions. Particularly, the 1,2-dimetalated aromatic compounds are very rare.

We herein attempt to trap polymetalated organometallic compounds inside supramolecular coordination capsules. Theoretically, flexible supramolecular capsules have good ability to adapt diverse substrates by adjusting cavity size. However, the use of flexible donor units in coordination self-assembly often causes a dilemma of yielding a mixture of multi-component self-assemblies. In this regard, inclusion of metal–metal interaction in the process of coordination self-assembly to facilitate the formation of a single discrete capsule structure may provide a solution. Metallophilic

[a]*The Key Laboratory of Bioorganic Phosphorus Chemistry & Chemical Biology (Ministry of Education), Department of Chemistry, Tsinghua University, Beijing 100084, China. E-mail: zhaolchem@mail.tsinghua.edu.cn*

[b]*Beijing National Laboratory for Molecular Sciences, State Key Laboratory of Rare Earth Materials Chemistry and Applications, Institute of Theoretical and Computational Chemistry, College of Chemistry and Molecular Engineering, Peking University, Beijing 100871, China*

† Electronic supplementary information (ESI) available: Supporting figures, high-resolution ESI-MS, NMR, crystal refinement details and computational results. CCDC 1558954–1558956, 1558958–1558960, 1558963. For ESI and crystallographic data in CIF or other electronic format see DOI: 10.1039/c7sc04503d

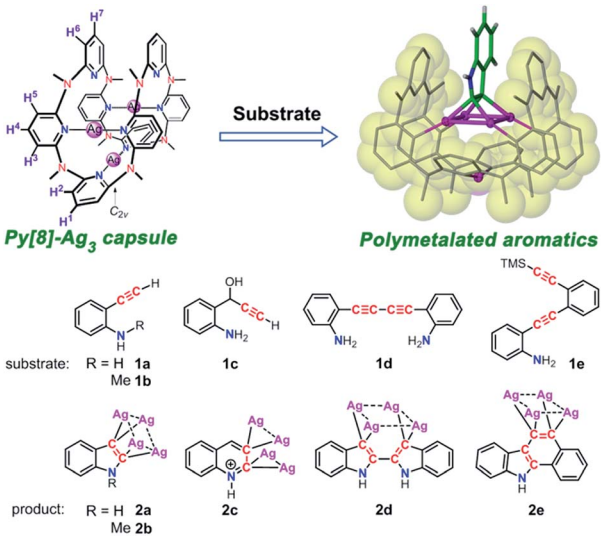

Scheme 1 Molecular structures of substrates and polysilver-bonded heteroaromatics formed within a metal–macrocycle capsule.

interaction as a kind of attractive interaction between metal atoms with closed-shell electronic configuration has been substantiated theoretically[11] and experimentally.[12] The well-known aurophilic and argentophilic interactions have been extensively observed in a number of polynuclear cluster compounds.[13–15] In addition, Au(I) and Ag(I) as a linear bridging unit were frequently applied in the construction of coordination cycles and cages.[16,17] In this work, we report the dynamic feature of a silver(I)-involved coordination capsule that is constructed by coordination-driven molecular folding of a flexible macrocyclic ligand octamethylazacalix[8]pyridine (**Py[8]**). The dynamic coordination capsule can trigger a one-step or cascade cyclization transformation for various alkynyl substrates with structural diversity (**1a–1e**), leading to successful isolation of unprecedented polysilver intermediates (**2a–2e**) of four heteroaromatics, including indole, quinoline, 2,2′-biindole, and benzocarbazole (Scheme 1). Single crystal X-ray diffraction analysis reveals that the macrocycle-based capsule structure provides optimal confined space to stabilize the elusive polymetalated aromatic intermediates. Computational studies indicate that metal-perturbed aromaticity and Ag_2–$C_{(sp^2)}$ multi-centered bonding both contribute to stabilization of the polysilver heteroaromatic complexes.

Results and discussion

Our recent work has shown that **Py[8]** can bind three silver atoms to construct a capsule-shaped crystalline complex $[Ag_3(\mathbf{Py[8]})(CF_3SO_3)][(CF_3SO_3)_2$ (**Py[8]-Ag$_3$**).[18] Interestingly, the metal ion binding process of **Py[8]** exhibited a significant cooperative coordination effect. ^{1}H NMR monitoring[18] and electrospray ionization mass spectroscopy (ESI-MS) (see Fig. S1 in the ESI† for details) revealed the formation of **Py[8]-Ag$_3$** even under metal ion deficient condition. Fitting of UV-vis titration results gave a large K_{a1} ($(1.66 \pm 0.17) \times 10^5$ M^{-1}) and K_{a3} ($(1.58 \pm 0.16) \times 10^5$ M^{-1}) relative to a small K_{a2} ($(1.90 \pm 0.19) \times 10^4$ M^{-1}) in the three-step metal ion binding process (Fig. S2†). This result rationalizes the ready formation of the 1 : 3 product **Py[8]-Ag$_3$** upon the presence of deficient silver(I) ions, and indicates that **Py[8]** helps the gathering of silver(I) ions by cooperative coordination effect.[19] Furthermore, structural characterization by variable temperature ^{1}H NMR uncovered a dynamic feature of the **Py[8]-Ag$_3$** coordination capsule. At room temperature ^{1}H NMR spectrum of **Py[8]-Ag$_3$** exhibited two sets of broad signals corresponding to the pyridyl β- and γ-protons of **Py[8]** (Fig. 1). Upon lowering the temperature from 293 to 213 K, the signals turned into a series of sharp peaks, which can be properly assigned to seven kinds of pyridyl hydrogen atoms as shown in **Py[8]-Ag$_3$** (Scheme 1). These results indicate that at low temperature the conformation of **Py[8]-Ag$_3$** is fixed as a rigid form while at room temperature many possible conformations dynamically interconvert.

The remarkable dynamic feature of the **Py[8]-Ag$_3$** capsule makes it as a unique flexible molecular flask to conduct organic transformations of diverse substrates. We purposefully selected several alkynyl substrates as **Py[8]** has been previously utilized by us as an outer template to realize controllable synthesis of silver acetylide clusters.[20] In order to guarantee quantitative construction of **Py[8]-Ag$_3$**, over three equivalents silver triflate were herein employed to react with **Py[8]**. Treatment of *o*-ethynylaniline (**1a**) with a CH_2Cl_2/CH_3OH (v/v 1 : 1) solution of **Py[8]-Ag$_3$** and additional silver triflate resulted in the occurrence of an intramolecular cyclization, finally yielding a polymetalated indole complex **2a** by crystallization. **2a** represents the first structurally well-defined organosilver intermediate for silver(I)-involved cyclizations of aminoalkyne derivatives.[21] Single-crystal X-ray diffraction showed that the indole ring in **2a** is negatively charged at two vicinal carbon atoms, and the resulting dianionic indole is stabilized by a coplanar Ag_4 rectangle (Fig. 2).

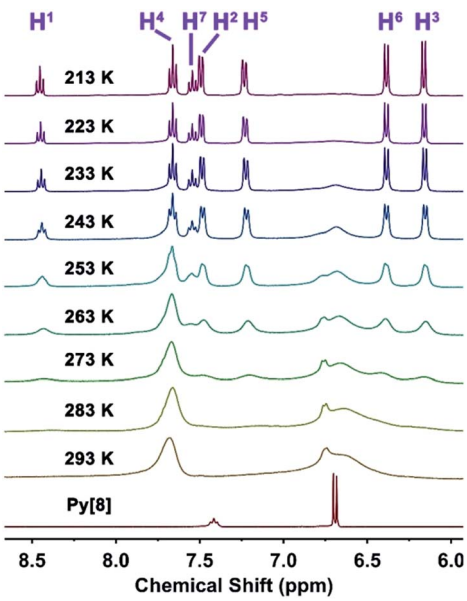

Fig. 1 Variable temperature ^{1}H NMR spectra of Py[8]-Ag$_3$. ^{1}H NMR spectrum of Py[8] at room temperature is plotted for comparison.

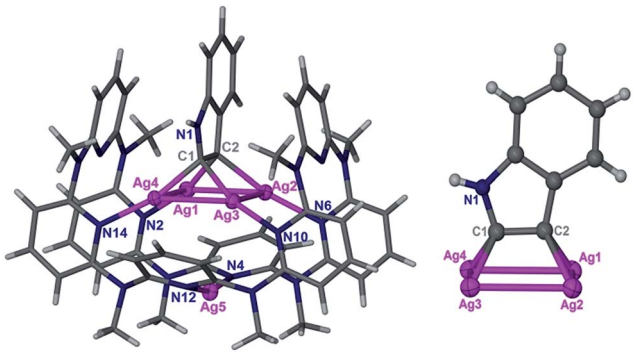

Fig. 2 Crystal structures of polysilver indole complex **2a** and its polymetalated core. Peripheral $CF_3SO_3^-$ anions and solvent molecules are omitted for clarity. Color coding: Ag, purple (ellipsoids set at 50% probability); C, gray; H, white; N, blue.

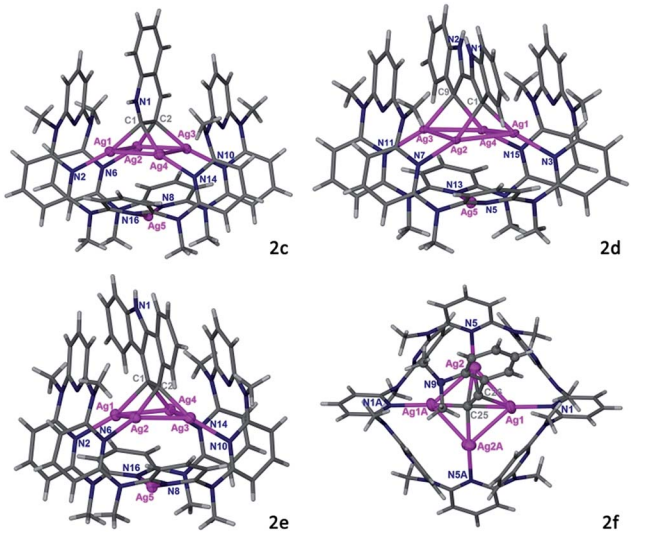

Fig. 3 Crystal structures of polymetalated aromatic complexes **2c–2e** and **Py[8]**-encircled silver acetylide cluster complex **2f**. All counter anions $CF_3SO_3^-$ and solvent molecules are omitted for clarity. Color coding: Ag, purple (ellipsoids set at 50% probability); C, gray; H, white; N, blue.

This argentophilic[12d] interaction-based tetrasilver rectangle is composed of two long edges (Ag_1–Ag_4: 3.093(2) Å, Ag_2–Ag_3: 3.085(2) Å) and two short ones (Ag_1–Ag_2: 2.831(2) Å, Ag_3–Ag_4: 2.831(2) Å). Each anionic carbon center is in an unusual pseudo-tetrahedral bonding fashion to connect with a short Ag–Ag edge (Ag–C: 2.06(2)–2.16(2) Å) and the neighboring nitrogen and carbon atoms. In addition, the planar indole ring is perpendicular to the Ag_4 rectangle. **Py[8]** in **2a** adopts a semi-open bowl-shaped conformation with a large cavity to accommodate the Ag_4 aggregate *via* four-fold Ag–N coordination (2.12(2)–2.21(2) Å). The bottom of the bowl is sealed by another silver atom. The **Py[8]-Ag$_3$** capsule-triggered cyclization is also applicable for the homolog substrate **1b**. The acquired tetrametalated indole complex **2b** is isostructural with **2a** (Fig. S3†). Interestingly, when **1a** was mixed with 4 equiv. $AgCF_3SO_3$ at room temperature without adding **Py[8]**, the ^{13}C NMR monitoring did not show any signal change for the C≡C moiety even after ten hours (Fig. S4†). Fourier transform infrared (FT-IR) spectra of the **1a**–$AgCF_3SO_3$ mixture exhibited a C≡C stretching vibration at 1999 cm^{-1} (Fig. S5†). The downward shift relative to **1a** (ν(C≡C) = 2096 cm^{-1}) is possibly due to the formation of a polynuclear cluster aggregate C≡CAg_n.[20]

We next investigated the transformation of substrate **1c** to study the selectivity of different cyclization modes within the coordination capsule. Previous studies have shown that **1c** preferred a 5-*exo-dig* cyclization to produce indole derivatives.[22] However, reaction of **1c** with the **Py[8]-Ag$_3$** capsule experienced a new 6-*endo-dig* cyclization pathway, finally producing a Ag_4-bonded quinoline ring in **2c** (Fig. 3). The **1c**-to-**2c** transformation should arise from intramolecular nucleophilic attack of an amino group on a C≡C group followed by aromatization-driven dehydration. The resulting quinoline ring is also doubly charged and each anionic carbon is bonded to a Ag–Ag edge. **Py[8]** adopts a similar bowl-shaped structure with a cavity to accommodate the quinoline–Ag_4 aggregate. It is noteworthy that the heterocyclic species in **2c** is in a quinolinium form. The composition of this unique structure has been substantiated by elemental analysis and ESI-MS (Fig. S6†). This quinolinium species has two resonance structures including the ylidic and carbene form as shown below, which were only reported in previous ruthenium carbonyl clusters of *N*-methylquinolin-3-yl-2-ylidene.[23] Since the Ag–C bond distances for two anionic carbon atoms in **2c** are comparable (2.163(8)–2.218(8) Å), we suppose that the heterocyclic skeleton in **2c** actually takes the ylidic form.

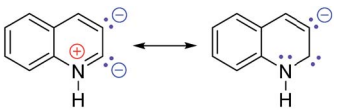

Ylidic form Carbene form

The **Py[8]-Ag$_3$** capsule-triggered cyclization was applicable to inner alkyne substrates as well. Reaction of substrate **1d** with **Py[8]-Ag$_3$** led to the construction of a 2,2′-biindole skeleton in **2d** through a two-step nucleophilic cyclization (Fig. 3). The 3,3′-positions of the biindole are both negatively charged, and each anionic carbon atom is bonded to two contacted silver atoms (Ag⋯Ag: 2.766(1)–2.775(1) Å) as similar as in **2a–2c**. Due to the large separation of two anionic carbon centers (C1⋯C9: 3.353 Å), the resulting tetrasilver aggregate in **2d** adopts a parallelogram shape rather than a rectangle in **2a–2c**. Consequently, the bowl-shaped **Py[8]** undergoes a significant expansion at open side to adaptively encircle the resulting 2,2′-biindole–Ag_4 organometallic cluster. Besides four alternate coordinative pyridines of **Py[8]** to support the Ag_4 aggregate as shown in **2a–2c**, in **2d** there are two more pyridine rings connecting with the Ag_4 parallelogram *via* longer Ag–N coordination (avg. 2.71 Å). In this way, the conformation of **Py[8]** in **2d** is fixed by the encapsulated Ag_4 parallelogram guest, finally leading to a well-resolved NMR spectrum. NMR monitoring showed that in the presence of **Py[8]-Ag$_3$** **1d** can be quantitatively transformed into **2d** within five hours (Fig. S7†).

Substrate **1e** was then attempted to construct a more complex and extended aromatic species within the capsule. As reported in literatures,[24] the trialkylsilyl-protected alkynyl group in **1e** is likely to undergo a silver(I)-induced desilylation to generate a terminal alkyne. When **1e** was mixed with **Py[8]-Ag$_3$**, it went through a cascade reaction pathway to produce a tetra-silver-bonded benzo[*a*]carbazole ring in **2e**, which is still encapsulated within a **Py[8]**-Ag bowl (Fig. 3). The newly constructed benzo[*a*]carbazole ring is supported by a Ag$_4$ rectangle through Ag–C bonding of two vicinal carbon atoms of a six-membered ring. This result indicates that the anionic carbon atom generated by the first cyclization of the inner alkyne species in **1e** has sufficient nucleophilicity to attack the Ag-activated ethynyl group to complete the second cyclization step. To the best of our knowledge, this is the first example of silver-catalyzed or -mediated cyclization toward the construction of an extended benzo[*a*]carbazole ring.

Above successful isolation of polysilver complexes of different heteroaromatics including fused, biaryl and extended polycyclic rings highlights the great potential of the **Py[8]**-based capsule structure to encapsulate various polymetalated guests. This extraordinary capability arises from the remarkable structural adjustment ability of **Py[8]**, which varies from its primitive planar parallelogram structure in crystalline state[25] to the curved ball-like conformation in **Py[8]-Ag$_3$**, and the bowl-shaped ones in **2a–2e**. With this in mind, we hypothesize that in the synthetic process of **2a–2e** the dynamic **Py[8]-Ag$_3$** capsule enables the silver atoms to flexibly partake in silver-acetylide bonding and then initiates the cyclization reaction. To prove this assumption, we employed substrate **1f**, which is an analog of **1a** but bearing a moderate nucleophilic group NMe$_2$, to react with **Py[8]-Ag$_3$**. The reaction finally generated an acetylide-centered Ag$_4$ cluster surrounded by a 1,2-alternate **Py[8]** macrocycle in **2f** (Fig. 3). We therefore conceive that the polymetallic gathering in **Py[8]-Ag$_3$** increases the effective concentration of silver ions and thus promotes the formation of a silver acetylide cluster inside **Py[8]**. Furthermore, the **Py[8]**-based capsule dynamically harnesses multiple coordination interactions to stabilize acquired polymetalated heteroaromatic species.

Previous studies have proved that organosilver complexes have limited stability.[26] However, complexes **2a–2e** are quite stable upon exposure to air and moisture. Preliminary reactivity studies revealed that reaction of **2a** with CF_3COOD gave rise to 2,3-deuterated indole in high yield, suggesting the nucleophilic nature of the Ag–C bonds. In solution, they can also keep their structures intact as evidenced in ESI-MS and NMR (Fig. S8–S18†). The pyridyl proton signals of **Py[8]** in **2a**, **2b**, **2c** and **2e** all gave very broad peaks, which can be ascribed to the interconversion of many possible fluxional conformations of **Py[8]** during the NMR time scale.[20] The NMR spectrum of the exceptional example **2d** contrarily exhibited a set of well-resolved peaks (Fig. S16†) because the conformation of **Py[8]** is fixed by the encapsulated Ag$_4$ parallelogram guest as mentioned above.

In order to comprehend the reasons for the excellent stability of **2a–2e**, we next carried out density functional theory (DFT) calculations to investigate the electronic structure and bonding

Table 1 Calculated multi-centered bond indices (MBI) and Mayer bond order in model complexes **2a′**, **2c′**, **2d′**, and **2e′**

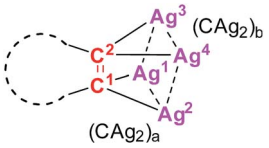

		2a′	**2c′**	**2d′**	**2e′**
MBI	$(CAg_2)_a$	0.0362	0.0706	0.0501	0.0463
	$(CAg_2)_b$	0.0343	0.0491	0.0557	0.0436
Mayer bond order	C^1–Ag^1	0.5631	0.5099	0.5323	0.6067
	C^1–Ag^2	0.5751	0.5416	0.5561	0.5463
	Ag^1–Ag^2	0.2128	0.3374	0.3067	0.2728
	C^2–Ag^3	0.5787	0.5743	0.6128	0.5887
	C^2–Ag^4	0.5666	0.5219	0.5551	0.5576
	Ag^3–Ag^4	0.2185	0.2795	0.2637	0.2774

of **2a**, **2c**, **2d**, and **2e**. In the calculated model complexes (denoted as **2a′**, **2c′**, **2d′**, and **2e′**, respectively), each coordinative pyridine ring of **Py[8]** was simplified to a 2,6-diaminopyridine. The calculated Mayer bond order results are summarized in Table 1. For model complex **2a′**, the sum of Ag–C bond orders for each CAg_2 species is larger than one. This result suggests that in addition to the donation *via* sp^2 orbital of each anionic carbon, the p_π orbital of the carbon also participates in bonding with two silver atoms. The inclusion of p_π orbital in Ag–C bonding is further confirmed by calculated molecular orbital (MO) diagrams (Fig. S19†). Furthermore, bond-order calculation of **2a′** revealed significant argentophilic interaction between two silver atoms (Table 1 and Fig. S20†), in good agreement with the short Ag···Ag distances in the crystal structure of **2a**. In addition, an interesting three-centered bond among the anionic carbon and two bonded silver atoms was observed in MO analysis (Fig. S21†). Multi-centered bond indices (MBI) calculation gave the values of 0.0362 and 0.0343 for two CAg_2 species in **2a′**, suggesting the existence of a multi-centered bond. The bond order and multi-centered bond index calculation of **2c′**, **2d′** and **2e′** also indicate the dominant presence of sp^2 and p_π electron donation and the multi-centered bond (Fig. S22–S29†).

The aromaticity of heterocyclic moieties in **2a′**, **2c′**, **2d′** and **2e′** was evaluated by nucleus-independent chemical shift (NICS) computations[27] (Fig. 4). As to **2a′**, the acquired NICS(1)$_{zz}$ values for both the five-(5MR) and six-membered ring (6MR) are −24.5 and −27.2 ppm, respectively, which are comparable with the values of an indole ring (−28.7 and −28.8 ppm, respectively). For other model complexes **2c′**, **2d′** and **2e′**, the calculated NICS values of the silver-bonded 5MR or 6MR are all negative, substantiating the aromatic nature of these rings. It is notable that the NICS values of the silver-bonded rings are less negative than other rings in the same heterocyclic skeleton, implying a lesser aromatic feature. This result can be rationalized by the above bond-order calculation, wherein p_π electron of the anionic carbon donates to silver atoms and thus lowers

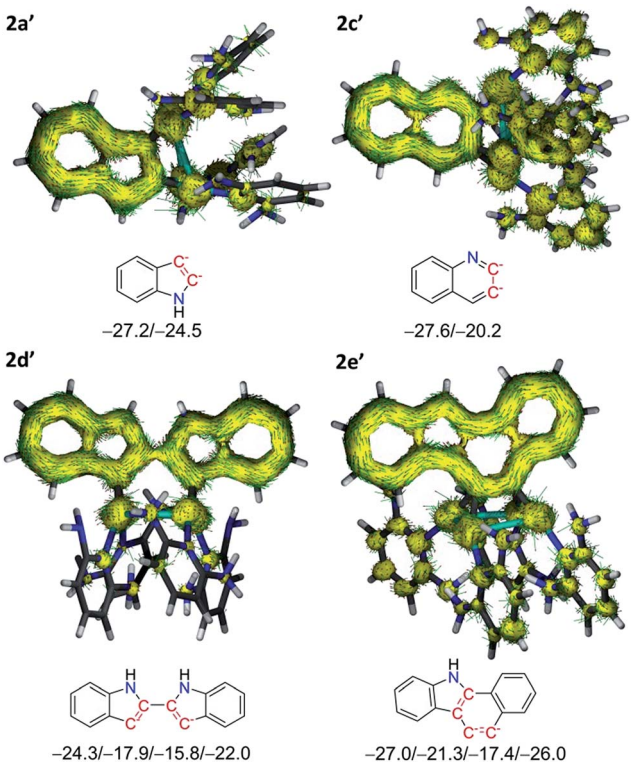

Fig. 4 ACID isosurfaces and NICS(1)$_{zz}$ values (p.p.m.) for six- and five-membered rings of **2a′**, **2c′**, **2d′** and **2e′** by the π contribution. Current density vectors are plotted onto the ACID isosurface of 0.03 to indicate dia- and para-tropic ring currents. The magnetic field vector is orthogonal with respect to the ring plane and points upward. The NICS(1)$_{zz}$ values are those computed at 1 Å above the geometrical centres of six- and five-membered rings.

aromaticity. Aromatic nature of the pseudo-tetrahedrally bonded heterocyclic rings in model complexes was further manifested by anisotropy of current-induced density (ACID) analysis.[28] In **2a′** and **2c′** (Fig. 4), the current density vectors plotted on the isosurface show a strong diatropic ring current in the π system. Similarly, the benzo[*a*]carbozole skeleton in **2e′** formed a large conjugation system with the diatropic ring current crossing along the rim of the whole skeleton. In **2d′**, the current is localized within only one of the two indole rings, suggesting the presence of two independent aromatic systems. The theoretical calculations substantiate that such polysilver-bonded heterocyclic rings in **2a–2e** are all aromatic although the anionic carbon atoms each is pseudo-tetrahedrally bonded with two silver atoms.

Conclusions

In conclusion, we have demonstrated that a macrocycle-based dynamic coordination capsule can trigger cyclization reactions for various alkyne substrates under mild conditions. In the presence of the dynamic coordination capsule, some unconventional reaction pathways for silver-mediated cyclizations (such as 6-*endo-dig* cyclization and cascade reaction) can be conducted. More importantly, several unprecedented polysilver complexes of four heteroaromatics, including indole, quinoline, 2,2′-biindole and benzocarbazole, have been successfully isolated and fully characterized. Theoretical analysis has revealed the presence of sp^2 and p_π electron donation and multi-centered bonding in the polysilver aromatic complexes, which substantiated the important role of metal-perturbed aromaticity in stabilization of the polysilver aromatic complexes. The present study showcases a promising approach to synthesize intricate organometallics by taking advantage of dynamic supramolecular capsule. Structure and reactivity comprehension of polymetalated organometallics may deepen our understanding of bonding nature and mechanistic studies, which is conducive to the advancement of more efficient and versatile synthetic methods. This study is still in progress.

Experimental

Materials and methods

All commercially available chemicals were used without further purification. Octamethylazacalix[8]pyridine (**Py[8]**) was synthesized according to the literature method by the [3 + 5] fragment coupling protocol between a terminal dibrominated linear trimer and a terminal diaminated linear pentamer.[25] The solvents used in this study were processed by standard procedures. ^{1}H and ^{13}C NMR experiments were carried out on a JEOL ECX-400 MHz instrument. Elemental analyses were recorded on a Thermo FlashEA 1112 elemental analyzer. Mass spectra were obtained using a Thermo Scientific Exactive Orbitrap instrument. Infrared spectra were recorded on a Perkin-Elmer spectrum 100 FT-IR spectrometer.

Synthesis of complexes 2a–2f

2a ($[Ag_5(C_8NH_5)(Py[8])](CF_3SO_3)_3$). In a 10 mL round-bottom flask, $AgCF_3SO_3$ (20.6 mg, 0.08 mmol) was dissolved in 2 mL CH_3OH at room temperature. To the solution was added **Py[8]** (17.0 mg, 0.02 mmol in 2 mL CH_2Cl_2). After ten minutes, a CH_2Cl_2 solution (0.5 mL) of substrate **1a** (2.3 mg, 0.02 mmol) was added dropwise. The mixture was further stirred for 10 hours. The solvent was then removed under vacuum to produce a crude oily product. Crystals of the polymetalated heteroaromatic compound **2a** were obtained by diffusion of diethyl ether into a concentrated mixed solution (CH_3OH : CH_2Cl_2 (v:v) = 1 : 1) of crude product. Yield: 46% (17.9 mg) based on **Py[8]**. When the amount of silver triflate was raised to 10 equivalents, the yield was enhanced to 72% (28.1 mg). Anal. calcd for **2a** ($C_{59}H_{53}Ag_5F_9N_{17}O_9S_3$): C, 36.33; H, 2.74; N, 12.21. Found: C, 35.96; H, 2.78; N, 12.57.

2b–2d. Synthetic procedures for complexes **2b–2d** are similar with that of **2a** using 10 equiv. silver triflate in the synthesis. **2b** ($[Ag_5(C_9NH_7)(Py[8])](CF_3SO_3)_3$): 25.5 mg, yield 65% based on **Py[8]**. Elemental analysis for **2b**·$3H_2O$ ($C_{60}H_{61}Ag_5F_9N_{17}O_{12}S_3$), found (calcd.): C, 35.36 (35.70); H, 2.72 (3.05); N, 11.49 (11.80). **2c** ($[Ag_5(C_9NH_5)H(Py[8])](CF_3SO_3)_4 \cdot 1.5CHCl_3 \cdot 0.75H_2O \cdot 0.5CH_3OH$): 26.7 mg, yield 68% based on **Py[8]**. Elemental analysis for **2c**·H_2O ($C_{61}H_{56}Ag_5F_{12}N_{17}O_{13}S_4$), found (calcd.): C, 34.22 (34.38); H, 2.65 (2.65); N, 11.05 (11.18). **2d** ($[Ag_5(C_{16}N_2H_{10})$(**Py**

[8])](CF$_3$SO$_3$)$_3$·2.5CH$_3$OH·Et$_2$O): 28.5 mg, yield 69% based on **Py[8]**. Elemental analysis for **2d** ($C_{67}H_{58}Ag_5F_9N_{18}O_9S_3$), found (calcd.): C, 38.87 (38.95); H, 2.83 (2.83); N, 12.09 (12.20).

2e–2f. In a 10 mL round-bottom flask, $AgCF_3SO_3$ (25.7 mg, 0.1 mmol) and $AgCF_3CO_2$ (22.0 mg, 0.1 mmol) were dissolved in CH_3OH (2 mL) at room temperature. To the mixture was added a CH_2Cl_2 solution (2 mL) of **Py[8]** (17.0 mg, 0.02 mmol). After stirred for ten minutes, a CH_2Cl_2 solution (0.5 mL) of **1e** or **1f** (0.02 mmol) was added dropwise. The mixture was stirred for further ten hours and the solvent was removed to give a crude oily product. Pale-yellow plate crystals were obtained by diffusion of diethyl ether into a concentrated mixed solution (CH_3OH : CH_2Cl_2 (v:v) = 1 : 1). **2e** ([$Ag_5(C_{16}NH_9)$(**Py[8]**)](CF$_3$SO$_3$)$_3$): 25.0 mg, 61% based on **Py[8]**. Elemental analysis for **2e**·CH_3OH ($C_{68}H_{61}Ag_5F_9N_{17}O_{10}S_3$), found (calcd.): C, 39.00 (39.21); H, 3.02 (2.95); N, 11.04 (11.43). **2f** ([$Ag_4(C_8NH_6)$(**Py[8]**)](CF$_3$SO$_3$)$_2$(CF$_3$CO$_2$)·2CH$_3$OH): 31.1 mg, 83% based on **Py[8]**. Elemental analysis for **2f** ($C_{61}H_{58}Ag_4F_9N_{17}O_9S_3$), found (calcd.): C, 39.49 (39.14); H, 3.34 (3.12); N, 12.48 (12.72).

X-ray crystallography

Single-crystal X-ray data for complexes **2a–2f** were collected at 173 K with Mo Kα radiation (λ = 0.71073 Å) on a Rigaku Saturn 724/724+ CCD diffractometer or Cu Kα radiation (λ = 1.54178 Å) on a Rigaku Oxford Diffraction SuperNova diffractometer. The selected crystal was mounted onto a nylon loop in polyisobutene and immersed in a low-temperature (173 K) stream of dry nitrogen gas during data collection. All structures were solved by direct methods, and non-hydrogen atoms were located from difference Fourier maps. Non-hydrogen atoms, otherwise noticed, were subjected to anisotropic refinement by full-matrix least-squares on F^2 by using the SHELXTL program[29] and Olex^2 program.[30] All figures were drawn by using X-seed program.[31] CCDC numbers for reported complexes are 1558954 (**2a** in space group *Cmcm*), 1558955 (**2a** in space group $P\bar{1}$), 1558956 (**2b**), 1558958 (**2c**), 1560 (**2d**), 1558959 (**2e**) and 1558963 (**2f**). The refinement details and crystal data for **2a–2f** are summarized in the ESI.†

Computational details

Theoretical calculations were performed using the Gaussian 09 program.[32] Initial structures of model clusters **2a′**, **2e′**, **2f′**, and **2g′** were obtained from crystal structures. The **Py[8]** ligand was simplified to four 2,6-diamino pyridines and the silver atoms not linked to the cluster core were omitted. All four structures were optimized at the TPSS level[33] of density functional theory with "Empirical Dispersion = GD3"[34] to describe the dispersion corrections. Furthermore, the frequency analyses were performed to confirm the characteristics of the calculated structures as minima. In the calculations, LanL2DZ basis set was used to describe the Ag atom, whereas the 6-31G(d) basis set for the C, N, and H atoms.[35] The NICS values were calculated at the TPSS-GIAO level.

Conflicts of interest

There are no conflicts to declare.

Acknowledgements

Financial support by National Natural Science Foundation of China (21522206, 21772111 and 21661132006) is gratefully acknowledged. We are grateful to Profs. Mei-Xiang Wang (THU), Sam C. K. Hau (HKBU), De-Xian Wang (ICCAS) and Han-Yuan Gong (BNU) for helpful discussions.

References

1 For recent reviews, see: (*a*) P. Ballester, M. Fujita and J. Rebek Jr, *Chem. Soc. Rev.*, 2015, **44**, 392, and other review articles in this theme issue; (*b*) A. Diaz-Moscoso and P. Ballester, *Chem. Commun.*, 2017, **53**, 4635.

2 For recent reviews, see: (*a*) M. Raynal, P. Ballester, A. Vidal-Ferran and P. W. N. M. van Leeuwen, *Chem. Soc. Rev.*, 2014, **43**, 1734; (*b*) D. Zhang, A. Martinez and J.-P. Dutasta, *Chem. Rev.*, 2017, **117**, 4900.

3 For reviews, see: (*a*) T. R. Cook and P. J. Stang, *Chem. Rev.*, 2015, **115**, 7001; (*b*) K. Harris, D. Fujita and M. Fujita, *Chem. Commun.*, 2013, **49**, 6703; (*c*) M. J. Wiester, P. A. Ulmann and C. A. Mirkin, *Angew. Chem., Int. Ed.*, 2011, **50**, 114; (*d*) C. J. Brown, F. D. Toste, R. G. Bergman and K. N. Raymond, *Chem. Rev.*, 2015, **115**, 3012; (*e*) A. J. McConnell, C. S. Wood, P. P. Neelakandan and J. R. Nitschke, *Chem. Rev.*, 2015, **115**, 7729; (*f*) L.-J. Chen, H.-B. Yang and M. Shionoya, *Chem. Soc. Rev.*, 2017, **46**, 2555.

4 (*a*) M. Yoshizawa, M. Tamura and M. Fujita, *Science*, 2006, **312**, 251; (*b*) Y. Inokuma, S. Yoshioka and M. Fujita, *Angew. Chem., Int. Ed.*, 2010, **49**, 8912.

5 C. J. Hastings, M. D. Pluth, R. G. Bergman and K. N. Raymond, *J. Am. Chem. Soc.*, 2010, **132**, 6938.

6 (*a*) M. Yoshizawa, Y. Takeyama, T. Kusukawa and M. Fujita, *Angew. Chem., Int. Ed.*, 2002, **41**, 1347; (*b*) N. Vallavoju and J. Sivaguru, *Chem. Soc. Rev.*, 2014, **43**, 4084.

7 (*a*) D. M. Kaphan, M. D. Levin, R. G. Bergman, K. N. Raymond and F. D. Toste, *Science*, 2015, **350**, 1235; (*b*) M. D. Levin, D. M. Kaphan, C. M. Hong, R. G. Bergman, K. N. Raymond and F. D. Toste, *J. Am. Chem. Soc.*, 2016, **138**, 9682.

8 A. M. Lifschitz, M. S. Rosen, C. M. McGuirk and C. A. Mirkin, *J. Am. Chem. Soc.*, 2015, **137**, 7252.

9 L. Ilies, M. Isomura, S. Yamauchi, T. Nakamura and E. Nakamura, *J. Am. Chem. Soc.*, 2017, **139**, 23.

10 C. H. Winter, K. N. Seneviratne and A. Bretschneider-hurley, *Comments Inorg. Chem.*, 1996, **19**, 1.

11 (*a*) P. Pyykkö, *Chem. Rev.*, 1997, **97**, 597; (*b*) P. Pyykkö, *Angew. Chem., Int. Ed.*, 2002, **41**, 3573; (*c*) P. Pyykkö, *Angew. Chem., Int. Ed.*, 2004, **43**, 4412.

12 (*a*) H. Schmidbaur and A. Schier, *Chem. Soc. Rev.*, 2008, **37**, 1931; (*b*) S. Sculfort and P. Braunstein, *Chem. Soc. Rev.*, 2011, **40**, 2741; (*c*) H. Schmidbaur and A. Schier, *Chem.*

Soc. Rev., 2012, **41**, 370; (*d*) H. Schmidbaur and A. Schier, *Angew. Chem., Int. Ed.*, 2015, **54**, 746.

13 (*a*) M. C. Gimeno and A. Laguna, *Chem. Soc. Rev.*, 2008, **37**, 1952; (*b*) A. Laguna, T. Lasanta, J. M. Lopez-de-Luzuriaga, M. Monge, P. Naumov and M. E. Olmos, *J. Am. Chem. Soc.*, 2010, **132**, 456; (*c*) T. Lasanta, M. E. Olmos, A. Laguna, J. M. Lopez-de-Luzuriaga and P. Naumov, *J. Am. Chem. Soc.*, 2011, **133**, 16358.

14 (*a*) L.-Y. Yao, F. K.-W. Hau and V. W.-W. Yam, *J. Am. Chem. Soc.*, 2014, **136**, 10801; (*b*) L.-Y. Yao and V. W.-W. Yam, *J. Am. Chem. Soc.*, 2015, **137**, 3506.

15 (*a*) S. C. K. Hau, M. C.-L. Yeung, V. W.-W. Yam and T. C. W. Mak, *J. Am. Chem. Soc.*, 2016, **138**, 13732; (*b*) Y.-P. Xie, J.-L. Jin, G.-X. Duan, X. Lu and T. C. W. Mak, *Coord. Chem. Rev.*, 2017, **331**, 54.

16 N. Sinha and F. E. Hahn, *Acc. Chem. Res.*, 2017, **50**, 2167.

17 (*a*) D. L. Reger, R. F. Semeniuc and M. D. Smith, *Inorg. Chem.*, 2003, **42**, 8137; (*b*) C. Khin, A. S. K. Hashmi and F. Rominger, *Eur. J. Inorg. Chem.*, 2010, 1063; (*c*) Q. Chen, F. Jiang, D. Yuan, G. Lyu, L. Chen and M. Hong, *Chem. Sci.*, 2014, **5**, 483.

18 X. He, X.-B. Xu, X. Wang and L. Zhao, *Chem. Commun.*, 2013, **49**, 7153.

19 G. Ercolani and L. Schiaffino, *Angew. Chem., Int. Ed.*, 2011, **50**, 1762.

20 (*a*) C.-Y. Gao, L. Zhao and M.-X. Wang, *J. Am. Chem. Soc.*, 2011, **133**, 8448; (*b*) C.-Y. Gao, L. Zhao and M.-X. Wang, *J. Am. Chem. Soc.*, 2012, **134**, 824; (*c*) X. He, C.-Y. Gao, M.-X. Wang and L. Zhao, *Chem. Commun.*, 2012, **48**, 10877.

21 B. C. J. van Esseveldt, F. L. van Delft, J. M. M. Smits, R. de Gelder, H. E. Schoemaker and F. P. J. T. Rutjesa, *Adv. Synth. Catal.*, 2004, **346**, 823.

22 Y. K. Kumar, G. R. Kumar, T. J. Reddy, B. Sridhar and M. S. Reddy, *Org. Lett.*, 2015, **17**, 2226.

23 J. A. Cabeza, I. del Río, E. Pérez-Carreño, M. G. Sánchez-Vega and D. Vázquez-García, *Angew. Chem., Int. Ed.*, 2009, **48**, 555.

24 U. Halbes-Letinois, J.-M. Weibel and P. Pale, *Chem. Soc. Rev.*, 2007, **36**, 759.

25 H.-Y. Gong, X.-H. Zhang, D.-X. Wang, H.-W. Ma, Q.-Y. Zheng and M.-X. Wang, *Chem.–Eur. J.*, 2006, **12**, 9262.

26 B. K. Tate, A. J. Jordan, J. Bacsa and J. P. Sadighi, *Organometallics*, 2017, **36**, 964, and references therein.

27 (*a*) P. v. R. Schleyer, C. Maerker, A. Dransfeld, H. Jiao and N. J. R. v. E. Hommes, *J. Am. Chem. Soc.*, 1996, **118**, 6317; (*b*) H. Fallah-Bagher-Shaidaei, C. S. Wannere, C. Corminboeuf, R. Puchta and P. v. R. Schleyer, *Org. Lett.*, 2006, **8**, 863.

28 (*a*) R. Herges and D. Geuenich, *J. Phys. Chem. A*, 2001, **105**, 3214; (*b*) D. Geuenich, K. Hess, F. Kçhler and R. Herges, *Chem. Rev.*, 2005, **105**, 3758.

29 G. M. Sheldrick, *Acta Crystallogr., Sect. A: Found. Crystallogr.*, 2008, **64**, 112.

30 O. V. Dolomanov, L. J. Bourhis, R. J. Gildea, J. A. K. Howard and H. Puschmann, *J. Appl. Crystallogr.*, 2009, **42**, 339.

31 J. L. Atwood and L. J. Barbour, *Cryst. Growth Des.*, 2003, **3**, 3.

32 M. J. Frisch, G. W. Trucks, H. B. Schlegel, G. E. Scuseria, M. A. Robb, J. R. Cheeseman, G. Scalmani, V. Barone, B. Mennucci, G. A. Petersson, H. Nakatsuji, M. Caricato, X. Li, H. P. Hratchian, A. F. Izmaylov, J. Bloino, G. Zheng, J. L. Sonnenberg, M. Hada, M. Ehara, K. Toyota, R. Fukuda, J. Hasegawa, M. Ishida, T. Nakajima, Y. Honda, O. Kitao, H. Nakai, T. Vreven, J. A. Montgomery Jr, J. E. Peralta, F. Ogliaro, M. Bearpark, J. J. Heyd, E. Brothers, K. N. Kudin, V. N. Staroverov, T. Keith, R. Kobayashi, J. Normand, K. Raghavachari, A. Rendell, J. C. Burant, S. S. Iyengar, J. Tomasi, M. Cossi, N. Rega, J. M. Millam, M. Klene, J. E. Knox, J. B. Cross, V. Bakken, C. Adamo, J. Jaramillo, R. Gomperts, R. E. Stratmann, O. Yazyev, A. J. Austin, R. Cammi, C. Pomelli, J. W. Ochterski, R. L. Martin, K. Morokuma, V. G. Zakrzewski, G. A. Voth, P. Salvador, J. J. Dannenberg, S. Dapprich, A. D. Daniels, O. Farkas, J. B. Foresman, J. V. Ortiz, J. Cioslowski and D. J. Fox, *Gaussian 09, Revision A.02*, Gaussian, Inc., Wallingford CT, 2009.

33 J. M. Tao, J. P. Perdew, V. N. Staroverov and G. E. Scuseria, *Phys. Rev. Lett.*, 2003, **91**, 146401.

34 S. Grimme, J. Antony, S. Ehrlichn and H. Krieg, *J. Chem. Phys.*, 2010, **132**, 154104.

35 P. J. Hay and W. R. Wadt, *J. Chem. Phys.*, 1985, **82**, 299.